Contents lists available at SciOpen

Food Science and Human Wellness

journal homepage: https://www.sciopen.com/journal/2097-0765

China Food Publishing Co.

Elucidating the protective mechanisms of *Chenpi* against alcoholic liver injury through integrated analysis of biochemical markers, microbiome, and transcriptome

Yanfang Liao[a,b,1], Zhaoping Pan[b,1], Fuhua Fu[a,b], Mingfang Peng[a,b], Yanjiao Fu[a,b], Wenbin Xiao[b], Yang Shan[a,b,*], Jiajing Guo[a,b,*]

[a] *Longping Agricultural College, Hunan University, Changsha 410125, China*

[b] *Dongting Laboratory, Hunan Institute of Agricultural Product Processing and Quality Safety, Hunan Academy of Agricultural Sciences, Changsha 410125, China*

ARTICLE INFO

Article history:
Received 5 May 2025
Received in revised form 29 June 2025
Accepted 15 January 2026

Keywords:
Chenpi
Alcoholic liver injury
Microbiome
Transcriptome

ABSTRACT

Alcoholic liver injury (ALI) has emerged as a significant public health concern, necessitating the urgent identification of medicinal-food resources for its prevention and treatment. As a natural medicinal food resource, *Chenpi* (CHE) is rich in various flavonoid bioactive compounds and exhibits potential antioxidant, anti-inflammatory, and hepatoprotective effects. However, the effect and mechanism of CHE in preventing and improving ALI are not yet known. This study sought to elucidate CHE's hepatoprotective mechanisms in ALI from the biochemical markers, microbiome and transcriptome perspectives. Results showed that CHE ameliorated ALI by improving oxidative stress, inflammatory cytokines and liver function. 16S rRNA analysis revealed that CHE alleviated ALI pathological progression primarily by restoring gut microbiota composition. Transcriptomic analysis showed that CHE improved ALI mainly related to MAPK signaling pathway. Pearson correlation analysis revealed that *Candidatus_Saccharimonas*, *Turicibacter*, and *Clostridium_sensu_stricto*_1 play key roles in the process by which CHE ameliorates alcohol-induced inflammation and pathological angiogenesis. These findings revealed that CHE has the potential to be used as a functional food to prevent or improve ALI.

1. Introduction

Chenpi (CHE) refers to the dried, mature peel of *Citrus reticulata* Blanco and its cultivated varieties, classified within the Rutaceae family. Primarily produced in Xinhui, Jiangmen City, Guangdong , it holds a significant place in both traditional Chinese medicine and culinary culture, with a history spanning centuries. In the "Dietetic materia medica" of the Tang Dynasty of China, CHE can be combined with a variety of ingredients to make soups, congees and other health food. During the Tang Dynasty, CHE was commonly combined with various ingredients to prepare health-promoting foods such as soups and porridges. The Ming Dynasty text Lei Gong's Treatise on Processing of Medicinals also recorded that CHE enters the lung, liver, spleen, and stomach meridians, indicating its potential hepatoprotective effects. CHE exhibits significant biological activity, attributed to its diverse bioactive compounds, including hesperidin, tangeretin, and nobiletin[1]. CHE has anti-obesity, anti-diabetes, anti-cancer and other effects[2-4]. Therefore, the research on the physiological function of CHE has become a hot spot.

The widespread prevalence of alcohol culture has contributed to a rising incidence of alcohol-related metabolic disorders. Approximately

* Corresponding authors at: Longping Agricultural College, Hunan University, Changsha 410125, China.
E-mail address: sy6302@sohu.com (Y. Shan); guojiajing1986@163.com (J.J. Guo)
Peer review under responsibility of Beijing Academy of Food Sciences.

SciOpen Publishing services by Tsinghua University Press

http://doi.org/10.26599/FSHW.2026.9250939

400 million people worldwide suffer from alcohol use disorders, with 209 million dependent on alcohol. According to data released by the World Health Organisation in 2024, alcohol caused 2.6 million deaths in 2019, accounting for 4.7% of all deaths, with male fatalities reaching 2 million[5]. Alcohol passes through the mouth and degrades a small amount of alcohol in the gut, with the remainder acting on the liver[6]. The gut-liver axis denotes the bidirectional communication pathway between the intestines and the liver[7]. Alcohol disrupts the intestinal barrier, leading to dysbiosis of the microbiota. This allows gut microbiota and their harmful metabolites to enter the liver *via* the portal vein, activating hepatic immune cells and triggering inflammation and oxidative stress[8]. This process is a key driver in the progressive deterioration of liver damage. Prolonged excessive alcohol consumption progressively escalates the condition, advancing from initial fatty liver and hepatitis to liver fibrosis and cirrhosis. Ultimately, this may progress to hepatocellular carcinoma. Consequently, alcohol-related liver disease has emerged as a progressively significant public health burden worldwide. There are significant differences in the pathological mechanisms through which various natural products intervene in alcoholic liver injury (ALI). A systematic dissection of these divergent pathways facilitates the precise identification of bioactive molecules with superior targeting capabilities. To seek more effective liver protection strategies, this study was compared with our previous reports[9], and systematically evaluated the impact of CHE on ALI.

This study investigated the hepatoprotective mechanisms underlying CHE's ameliorative effects on ALI. A series of biochemical indicators such as oxidative stress, inflammatory response and resistance to liver injury were used to characterize the effects of CHE on ALI in mice. Transcriptome and microbiome analysis were performed on the livers of alcoholic liver-injured mice. We hope our study will offer theoretical groundwork for developing CHE-derived nutraceuticals against ALI.

2. Materials and methods

2.1 Preparation of CHE

CHE with a storage time of 3 years was provided by Xinhui, Jiangmen City, Guangdong. The aqueous CHE extract were prepared according to the literature, with a slight change[10]: Briefly, powdered CHE was subjected to triple boiling water extraction (1:20) with successive extraction durations of 20, 20, and 10 min. The combined extracts were concentrated under reduced pressure to obtain a final aqueous solution.

2.2 High performance liquid chromatography (HPLC) analysis

HPLC analysis was performed according to our previously established method[11]. A total of 1 g of CHE powder was extracted with 10 mL methanol *via* ultrasonication (50 °C, 30 min) followed by centrifugation (4 °C, 4 000 × *g*, 10 min). The extraction was repeated twice with methanol (10 mL each). Combined supernatants were transferred to a 50 mL volumetric flask and brought to volume with methanol, yielding the final sample solution. The sample solution was passed through a 0.22 μm organic filter prior to transfer into an HPLC vial for chromatographic analysis. Dual-wavelength detection was carried out at 330 and 283 nm.

2.3 Network pharmacological analysis

The active constituents of CHE were obtained from the TCMSP database by applying the screening thresholds of oral bioavailability (OB) ≥ 30% and drug-likeness (DL) ≥ 0.18. Additional active constituents were supplemented through a comprehensive literature review. The potential protein targets of these active constituents were predicted using Swiss Target Prediction with the organism set to *Homo sapiens*. Disease-associated targets were identified from the GeneCards and OMIM databases using the keyword "alcoholic liver injury". To improve transparency, we applied a relevance score cutoff of ≥ 10 in GeneCards. Genes retrieved from OMIM were used to enhance confidence in ALI relevance.The intersection of potential CHE targets and ALI-associated genes was identified using Venny 2.1.0 (https://bioinfogp.cnb.csic.es/tools/venny/), a web-based tool for visualizing overlaps. The common targets were subsequently uploaded to the STRING database, with parameters configured for "Homo sapiens" and an interaction score threshold of 0.90. Nodes with no connections were excluded from the protein-protein interaction (PPI) network. Interaction data were downloaded in TSV format and further examined using Cytoscape 3.10. Core protein targets with betweenness, closeness, and degree values above the median were identified, and the analysis was repeated in triplicate. Cytoscape was employed to construct a bioactive compound-target network of CHE against ALI. Kyoto Encyclopedia of Genes and Genomes (KEGG) pathway and Gene Ontology (GO) functional enrichment analyses of the targets were performed using DAVID database with Homo sapiens as the selected species.

2.4 Mice modeling and feeding

A total of 30 male C57BL/6J mice ((20 ± 2) g) were obtained from Hunan Slaike Jingda Experimental Animal Co., Ltd. (License No. SCXK (Xiang) 2019-0004) and housed in a specific-pathogen-free facility under controlled conditions[9]. Following a one-week acclimatization period, the mice were randomly assigned to 3 groups (n = 10 per group): control (CON), alcohol-treated (ALC), and CHE-treated. The mice received daily administrations twice per day, with a minimum interval of 6-h interval between treatments, according to their group assignment. The CON group received normal saline at both time points. The ALC group received ethanol (2.4 g/kg) in the morning, followed by normal saline in the afternoon. The CHE group received ethanol in the morning, followed by CHE (3 g/kg) in the afternoon. Body weights were recorded weekly throughout the 11-week experimental period. At termination, mice were anesthetized with ether until loss of consciousness, after which blood was collected *via* orbital puncture, and euthanasia was performed by cervical dislocation. As these experiments were performed simultaneously, the CON and ALC group animals data analyzed in this study (including body weight gain, biochemical markers, histological section, microbiome and transcriptome) were derived from our previously published work[9].

2.5 Measurement of biochemical markers

Serum aspartate aminotransferase (AST), alanine aminotransferase (ALT), tumor necrosis factor-α (TNF-α), and interleukin-6 (IL-6) and liver malondialdehyde (MDA), superoxide dismutase (SOD), catalase (CAT), glutathione peroxidase (GSH-PX), aldehyde dehydrogenase (ALDH) and alcohol dehydrogenase (ADH) were measured in accordance with the instructions formulated by Jiangsu Meimian industrial Co., Ltd. (Yancheng, China).

2.6 Histopathological observation

Histopathological examination of liver tissues was performed according to previously described methods[9]. Paraffin-embedded sections were deparaffinized and rehydrated, then frozen at –20 °C. After returning to room temperature, the sections were refixed and treated with HD constant staining pre-treatment solution prior to staining with hematoxylin and eosin (H&E). Finally, sections were mounted in neutral resin and examined under a Nikon Eclipse E100 microscope (Tokyo, Japan) for imaging.

2.7 Sequencing analysis of gut microbiota

Sequencing analysis was performed according to our previously published method, involving four major steps: DNA extraction from samples, PCR amplification, fluorescence-based quantification, and final sequencing on the Illumina platform[9,12].

2.8 Transcriptome analysis

Transcriptome profiling followed our published methodology[9,13]. In short, total RNA was isolated with the TRIzol (Invitrogen) method, followed by mRNA enrichment using Oligo(dT) magnetic beads and fragmentation in appropriate buffer. The fragmentation buffer is then added to the fragmentation buffer. cDNA synthesis was performed using random primers and reverse transcriptase, followed by end-repair to convert sticky ends into blunt ends for adaptor ligation. The ligated adaptor products are then screened for fragmentation and library enrichment and finally sequenced by Illumina.

2.9 Statistical analysis

Values represent mean ± SD. Biochemical marker data were analyzed using GraphPad Prism 8.0 (USA) for One-way analysis of variance. The transcriptomic and microbiomic data were analyzed using the Cloud Platform (https://www.majorbio.com). Differences were considered statistically significant at $P < 0.05$, $P < 0.01$, and $P < 0.001$.

3. Results

3.1 Key flavonoid analysis of CHE

The research results showed that the content of tangeretin was (138.5 ± 10.9) mg/100 g, nobiletin was (1 982.4 ± 17.7) mg/100 g, and the content of hesperidin was (2 831.55 ± 19.2) mg/100 g (Fig. 1). The HPLC chromatogram is provided in Fig. S1.

3.2 CHE improved ALI may be closely related to MAPK signaling pathway

Alcohol-related liver injury targets were collected from 2 distinct disease databases. GeneCards yielded 2 281 targets, while OMIM provided 35, with 26 targets overlapping between databases (Fig. 2A, Table S1). Potential therapeutic targets were identified through the TCMSP database and relevant literature, including the following bioactive compounds: tangeretin, hesperidin, sitosterol, naringenin, 5,7-dihydroxy-2-(3-hydroxy-4-methoxyphenyl)chroman-4-one, citromitin, and nobiletin (Fig. 2B). A total of 210 shared genes were obtained from the intersection of the targets of ALI and the targets of CHE (Figs. 2C and D). GO and KEGG enrichment analysis were conducted targeting the 210 core targets *via* the DAVID database. As illustrated in Fig. 2F, GO enrichment analysis revealed: (i) biological processes including ephrin receptor signaling pathway, positive regulation of phosphatidylinositol 3-kinase activity, and insulin-like growth factor receptor signaling pathway; (ii) cellular components comprising receptor complex, plasma membrane, and membrane raft; and (iii) molecular functions involving histone H2AXY142 kinase

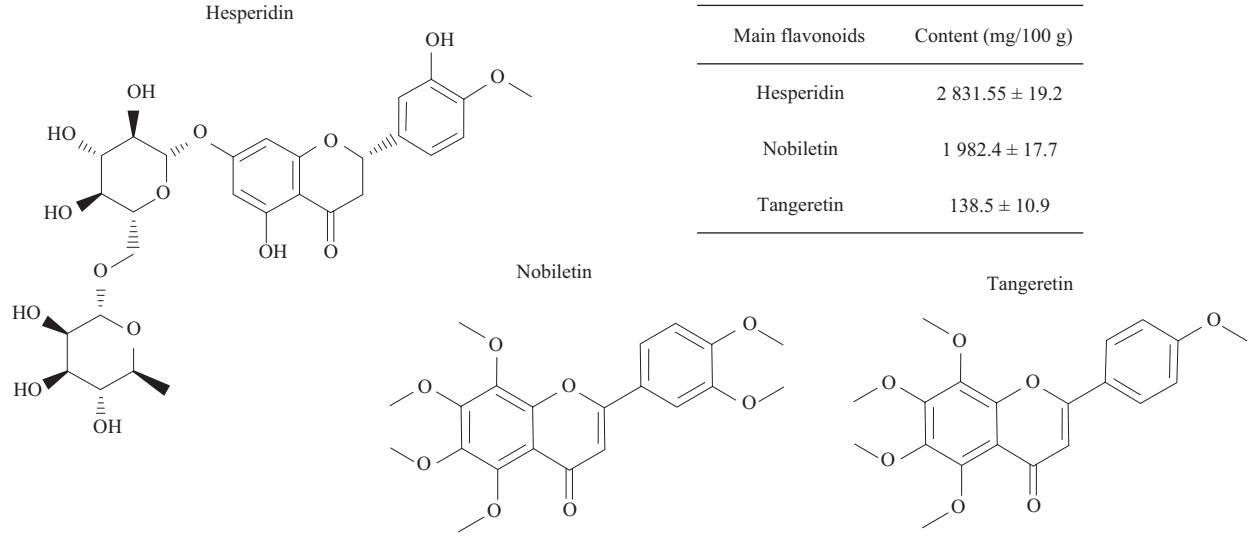

Main flavonoids	Content (mg/100 g)
Hesperidin	2 831.55 ± 19.2
Nobiletin	1 982.4 ± 17.7
Tangeretin	138.5 ± 10.9

Fig. 1 Structural formula and contents of three main flavonoids in CHE.

activity, histone H3Y41 kinase activity and protein tyrosine kinase activity. KEGG enrichment analysis showed that the molecular mechanisms underlying CHE in ameliorating alcohol-induced liver injury may involve multiple pathways, including: pathways in cancer, PI3K-Akt signaling pathway, proteoglycans in cancer, chemical carcinogenesis-reactive oxygen species, chemical carcinogenesis-receptor activation, and MAPK signaling pathway (Fig. 2G). The core genes of PPI were obtained by CytoNCA plug-in, which were *PIK3CA*, *HRAS*, *ESR1*, *PIK3R1*, *SRC*, and *AKT1* (Fig. 2E).

3.3 CHE improved oxidative stress, inflammation and liver injury

In terms of oxidative stress, The ALC group displayed a significant increase in MDA along with markedly reduced activities of hepatic antioxidant enzymes (SOD, CAT, and GSH-PX) compared to the CON group. However, CHE treatment effectively counteracted these changes. Regarding inflammatory response, alcohol consumption significantly elevated serum TNF-α and IL-6 levels, whereas CHE administration mitigated this effect. In terms of liver injury phenotypes, the ALC group showed elevated serum ALT and AST levels, which were notably decreased following CHE treatment. Moreover, liver histopathology demonstrated that CHE could reduce alcohol-induced inflammatory cell infiltration. Regarding alcohol metabolism enzymes levels, CHE has a tendency to alleviate alcohol metabolism enzymes, but it is not significant. In summary, CHE protects mice from ALI through antioxidant, anti-inflammatory and anti-liver damage (Fig. 3).

3.4 CHE improved gut microbiota dysbiosis in mice

PCoA based on Bray-Curtis distances and ANOSIM were performed at OTU level to evaluate differences in microbial community composition among groups. The CHE and CON groups were closer together, while the ALC group was the furthest away from the CON group (Fig. 4B). The data revealed differential community structures among groups, showing greater similarity between CHE and CON groups than with ALC. We subsequently employed various visualization methods to characterize these compositional differences. Overlapping analysis were used to identify shared and unique OTUs among the 3 groups. As shown in Fig. 4A, the three groups share 483 OTUs, with 597, 615 and 594 OTUs for the CON, ALC and CHE groups respectively. In addition, the CON, ALC and CHE groups have 22, 43 and 20 OTUs respectively. Bar plots illustrated

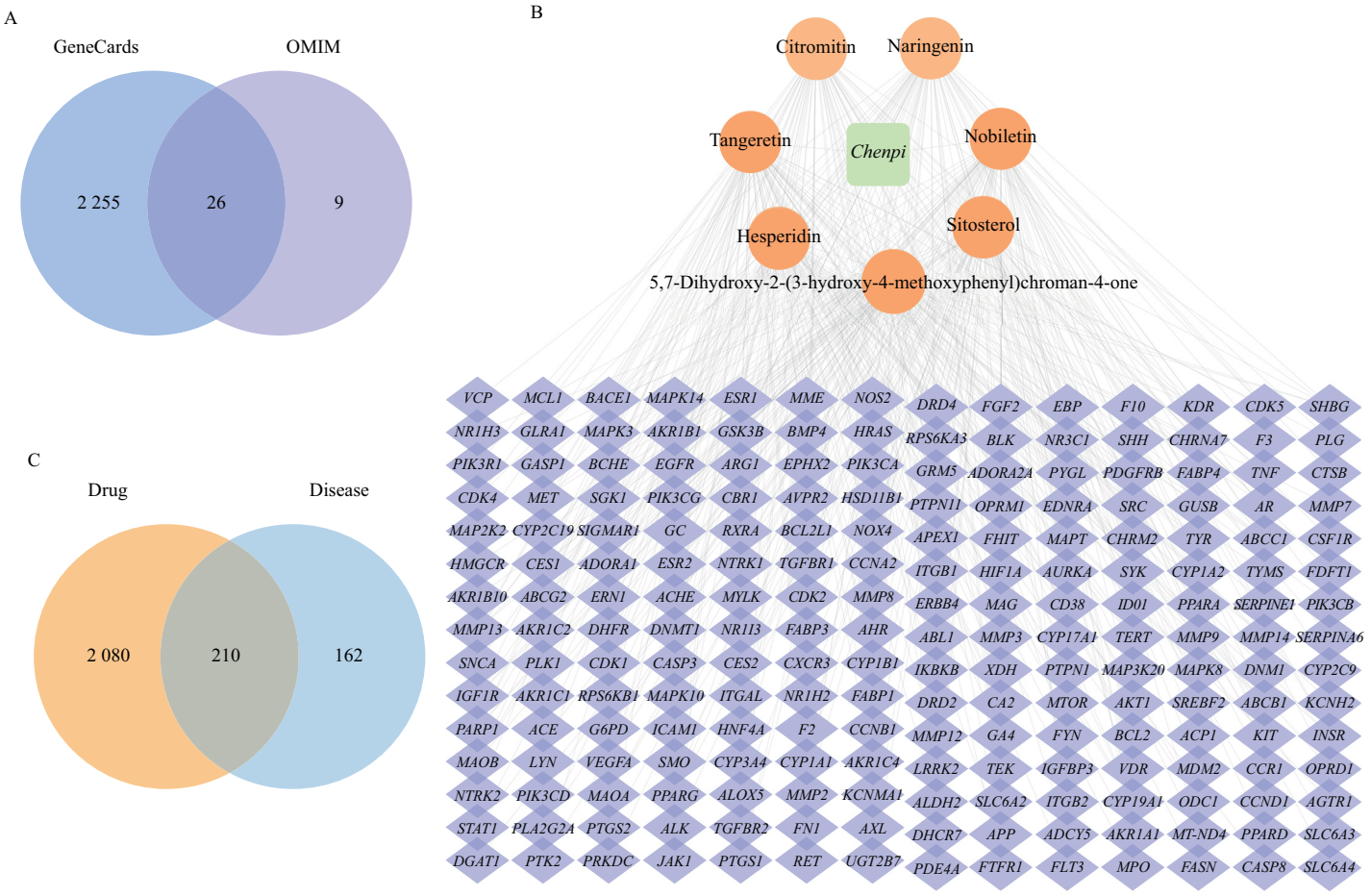

Fig. 2 Network pharmacological analysis of CHE for improving ALI. (A) Venn analysis of ALI-related targets in OMIM and GeneCards databases. (B) Network of CHE active components and ALI targets. (C) Intersection analysis of CHE active components and ALI targets. (D) PPI network of the 210 shared targets. (E) Core target identification. (F) GO enrichment analysis of the 210 common targets. (G) KEGG enrichment analysis of the 210 common targets.

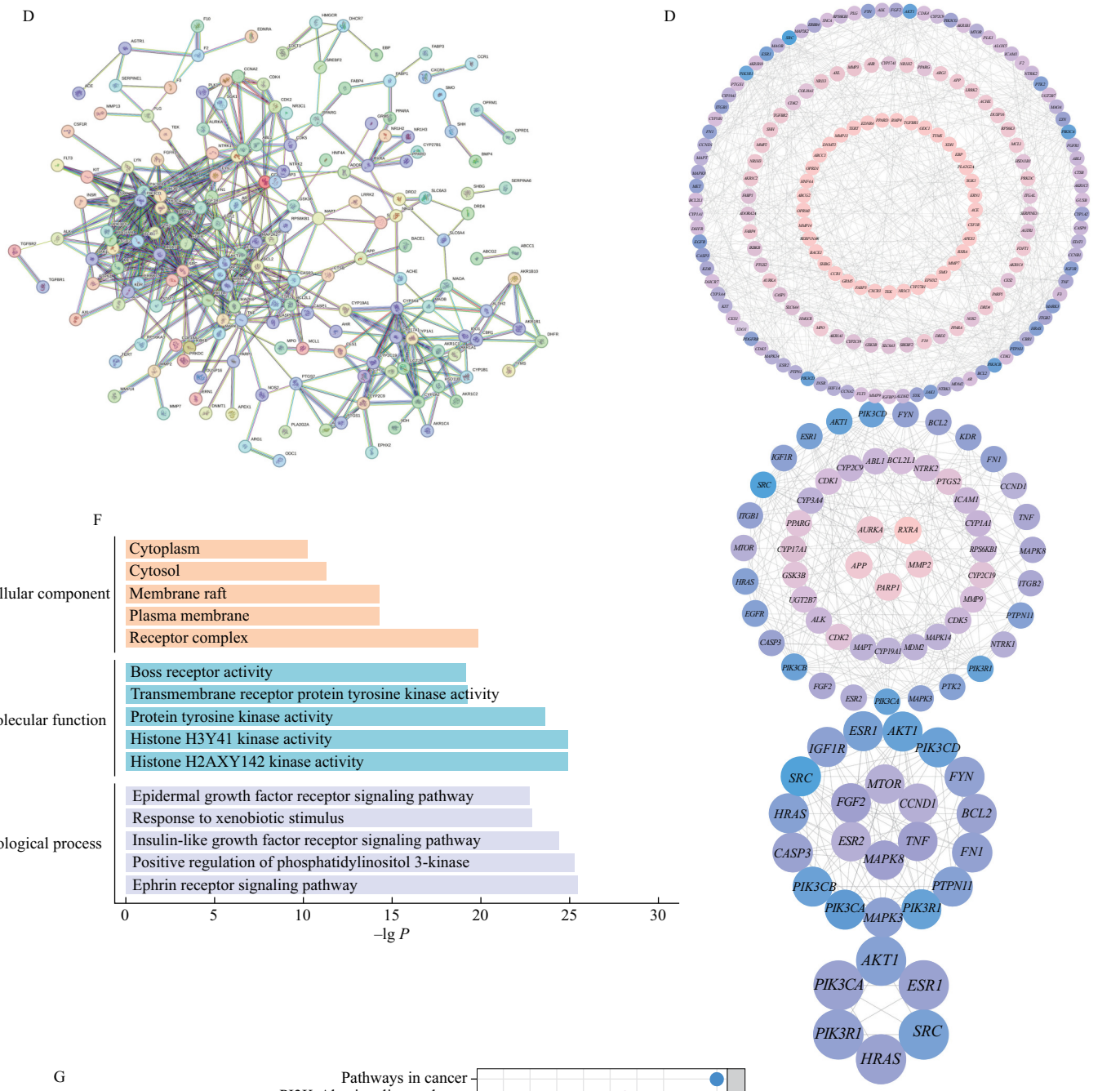

Fig. 2 (*Continued*)

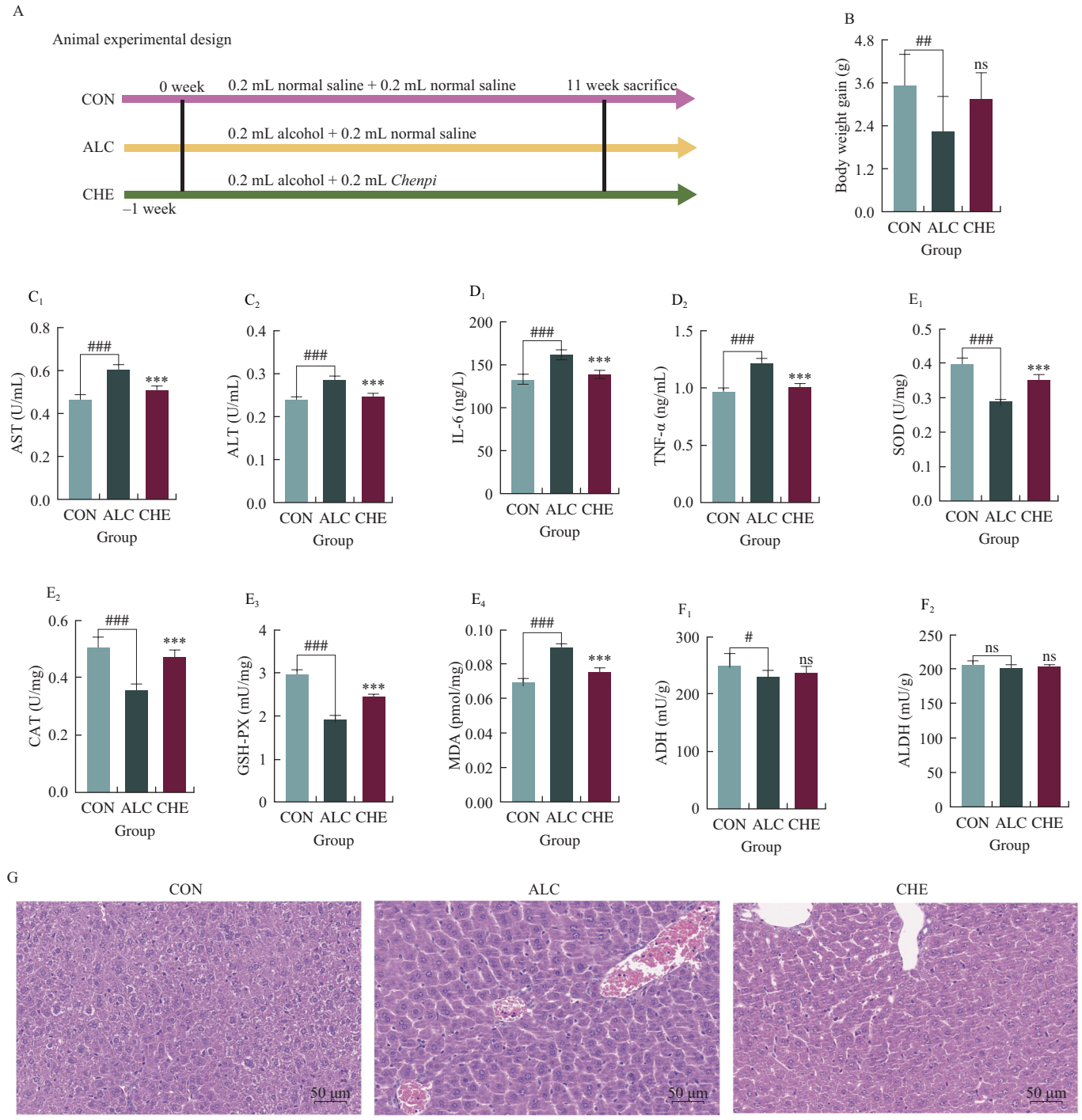

Fig. 3 The effect of CHE on drinking mice. (A) Experimental design of mice. (B) Body weight gain. (C) Liver injury factors. (D) Inflammatory factors. (E) Oxidative stress indexes. (F) Alcohol metabolism enzyme levels. (G) HE stained section of liver. All data were analyzed using GraphPad Prism 8.0 for One-way analysis of variance. $^{\#}P < 0.05$, $^{\#\#}P < 0.01$, $^{\#\#\#}P < 0.000\ 1$, ns not significant.

the dominant phyla and genera across groups (Figs. 4C and D). The CON group exhibited higher abundances of Bacteroidota, Firmicutes, and Deferribacterota, while ALC and CHE groups were enriched in Bacteroidota, Firmicutes, and Actinobacteriota (Fig. 4C). At the genus level, the CON group exhibited higher relative abundances of norank_f_Muribaculaceae, *Lactobacillus*, and *Mucispirillum*. In contrast, ALC and CHE groups showed predominance of norank_f_Muribaculaceae, Lachnospiraceae_NK4A136_group, and *Dubosiella* (Fig. 4D).

At the phylum level, CHE showed decreased Campilobacterota but increased Patescibacteria abundance relative to ALC (Fig. 4E). Genus-level analysis demonstrated higher abundance of *Alistipes*, *Candidatus_Saccharimonas*, *Faecalibaculum*, norank_f_norank_o_Clostridia_vadinBB60_group, and Coriobacteriaceae_UCG-002 in the CHE group ($P < 0.05$). Conversely, CHE exhibited lower levels of *Helicobacter*, *Turicibacter*, *Clostridium_sensu_stricto*_1, *Ruminococcus*, and *Eubacterium_xylanophilum*_group compared to ALC group ($P < 0.\ 05$, Figs. 4F and G).

3.5 CHE ameliorated ALI through modulation of the MAPK signaling pathway

To further explore the mechanism by which CHE exerts its effects on the liver of alcohol-exposed mice, we conducted transcriptomic analysis of liver tissues from the CHE and ALC groups. In this study, CHE and ALC groups obtained 10 365 and 10 676 genes, respectively, among which the 2 groups shared 10 084 genes, and CHE and ALC groups had 281 and 592 unique genes, respectively (Fig. 5A). The bar chart showed 364 differentially expressed genes (DEGs), including 98 up-regulated and 266 down-regulated (Figs. 5B and C). KEGG functional annotation showed that metabolism, environmental information processing, cellular processes, organismal systems and human diseases was involved in 1, 2, 2, 7 and 8 pathways, respectively (Fig. 5D). GO functional annotation identified that biological process, cellular component and molecular function were involved in 9, 7 and 4 pathways respectively (Fig. 5E). KEGG enrichment analysis revealed that the MAPK signaling pathway was the most significantly enriched in the CHE group (Fig. 5G, Table S2). A total of 19 differential genes were identified in the MAPK signaling pathway in this study, including *Mef2c*, *Tek*, *Epha2*, *Mapt*, *Flt4*, *Gadd45g*, *Rps6ka2*, *Hgf*, *Flt1*, *Map3k13*, *Hspa2*, *Kdr*, *Rasgrp3*, *Hspa1b*, *Hspa1a*, *Nr4a1*, *Fos*, *Il1b* and *Cacng7* (Fig. 5H). GO enrichment analysis revealed predominant enrichment of upregulated DEGs in muscle contraction, muscle system processes, and ion binding (Fig. 5F, Table S2). GO enrichment analysis highlighted predominant enrichment of downregulated DEGs in regulation of angiogenesis, enzyme linked receptor protein signaling pathway, cell adhesion, positive regulation of protein phosphorylation, regulation of cell adhesion and regulation of vasculature development (Fig. 5F, Table S2).

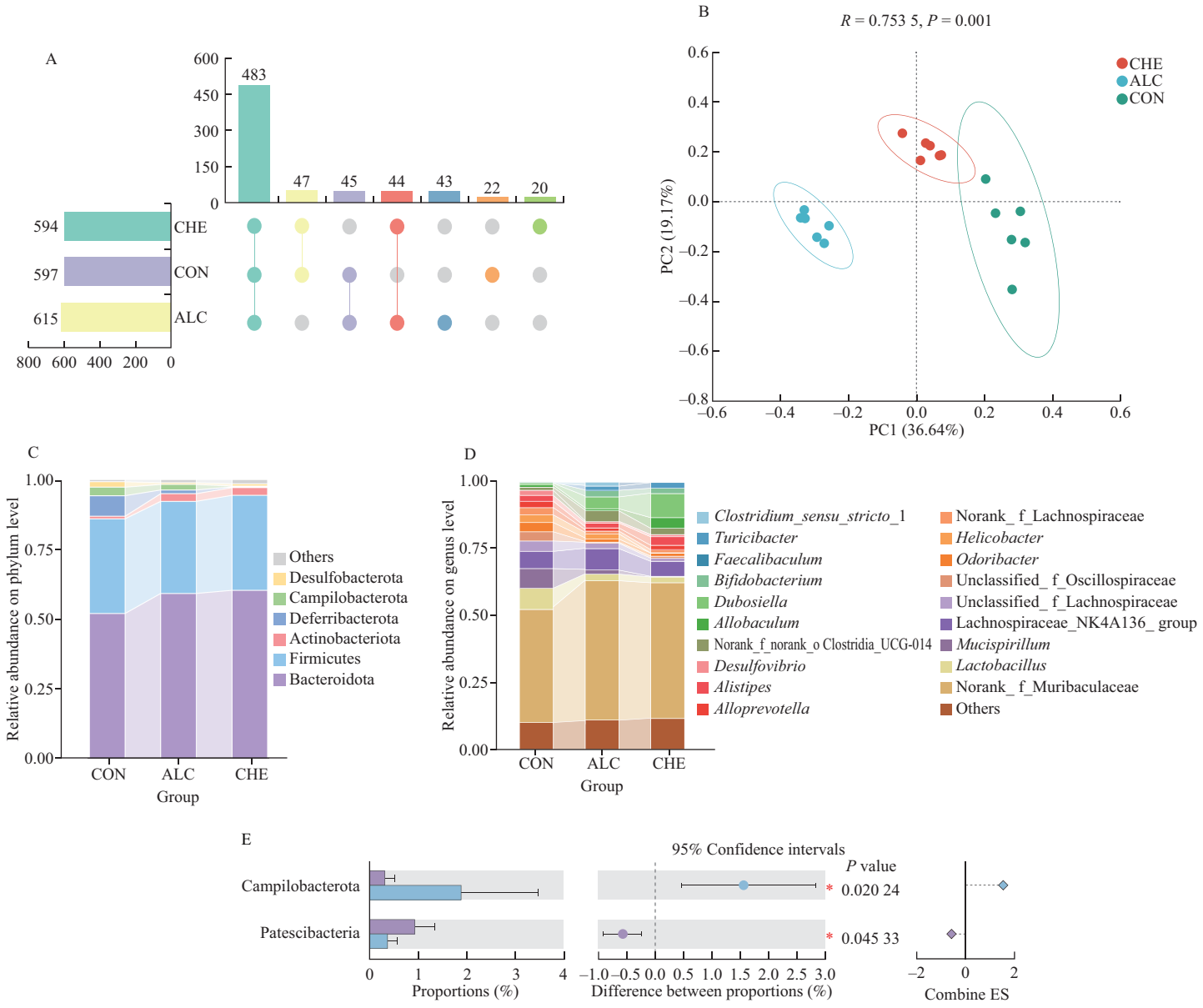

Fig. 4 Gut microbiota analysis. (A) Overlapping analysis. (B) PCoA on OTU level. (C) Community composition of gut microbiota at phylum level. (D) Community composition of gut microbiota at genus level. (E) Bar plots display the phylum-level distribution of gut microbiota in CHE and ALC groups (95% CI). (F) Bar plots display the genus-level distribution of gut microbiota in CHE and ALC groups (95% CI). (G) Kruskal-Wallis H test was used to compare the relative abundance of some bacteria between CON, ALC and CHE groups.

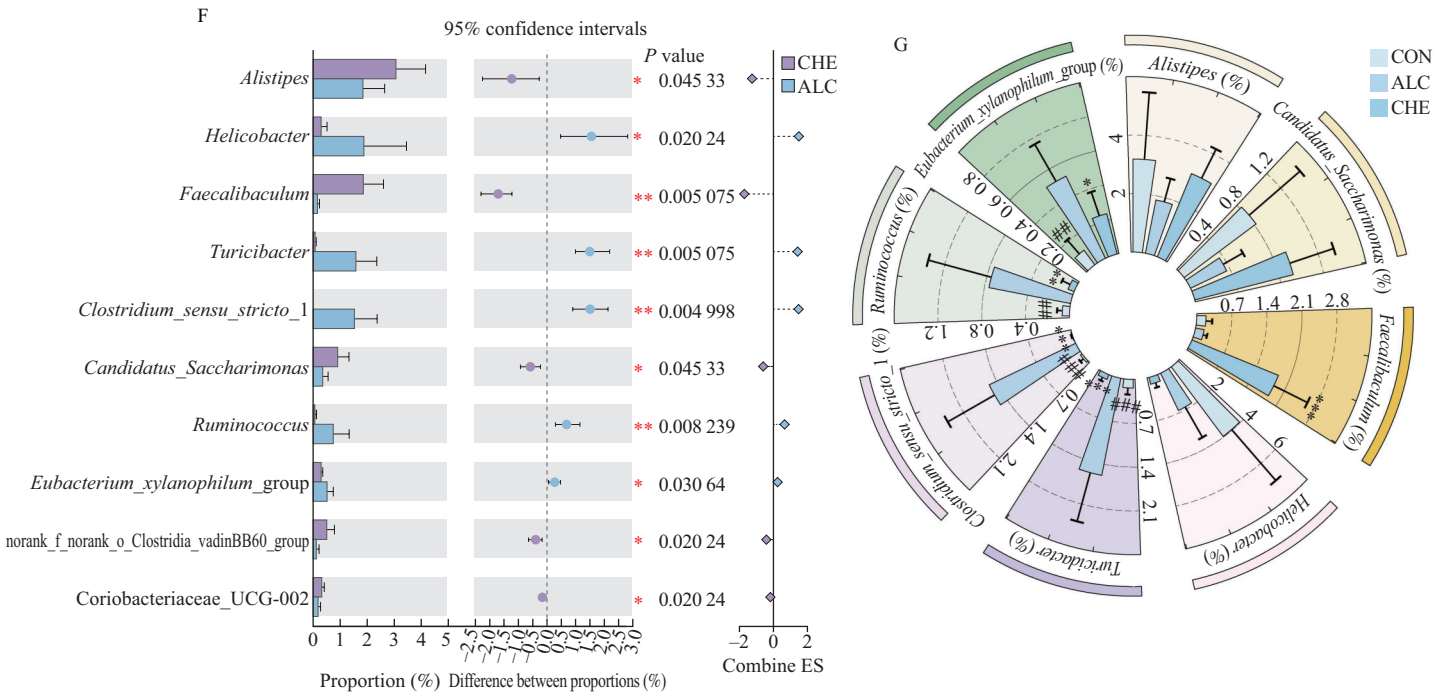

Fig. 4 (*Continued*)

3.6 Correlation analysis of BM and MT

To visualize the role of gut microbiota, pearson correlations were performed to assess relationships between gut microbiota and biochemical markers (IL-6, TNF-α, MDA, SOD, ALT, AST, GSH-PX, and CAT). Genus-level microbiota showed significant correlations with multiple biochemical markers. Notably, *Faecalibaculum*, *Turicibacter*, *Clostridium_sensu_stricto*_1, *Candidatus_Saccharimonas* each correlated with eight biochemical markers, while norank_f_norank_o_Clostridia_vadinBB60_group showed associations with 7. *Faecalibaculum* and *Candidatus_Saccharimonas* showed inverse relationships with TNF-α, IL-6, MDA, ALT, and AST levels, while being positively linked to the antioxidant markers SOD, GSH-PX, and CAT ($P < 0.05$). In contrast, *Turicibacter* and *Clostridium_sensu_stricto*_1 were positively correlated with TNF-α, MDA, ALT, and AST, but negatively associated with SOD, GSH-PX, and CAT ($P < 0.05$). *Alistipes* was significantly positively related to SOD and GSH-PX, whereas it showed negative correlations with TNF-α, ALT, and MDA ($P < 0.05$). Additionally, *Helicobacter* was positively correlated with both MDA and AST ($P < 0.05$). *Ruminococcus* demonstrated a significant negative correlation with GSH-PX and positive correlations with IL-6, TNF-α, MDA, and AST ($P < 0.05$). Moreover, the *Eubacterium_xylanophilum*_group displayed significant positive associations with TNF-α and MDA ($P < 0.05$; Fig. 6A).

Turicibacter, *Clostridium_sensu_stricto*_1, *Candidatus_Saccharimonas*, *Muribaculum* and *Ruminococcus* had the highest number of genes associated 9, 8, 9, 9 and 10 respectively. *Turicibacter* showed significant positive correlations with *Hgf*, *Rasgrp3*, *Mapt*, *Gadd45g*, *Hspa2*, *Tek, Flt1*, and *Kdr*, while exhibiting a negative association with *Il1b*. *Clostridium_sensu_stricto*_1 showed positive correlations with *Hgf*, *Rasgrp3*, *Mapt*, *Gadd45g*, *Hspa2, Tek*, and *Flt1*, but was negatively associated with *Il1b*. *Candidatus_Saccharimonas* showed positive correlations with *Map3k13*, *Epha2*, *Hspa2*, *Tek*, *Flt4*, *Rps6ka2*, *Flt1*, and *Kdr*, but was negatively correlated with

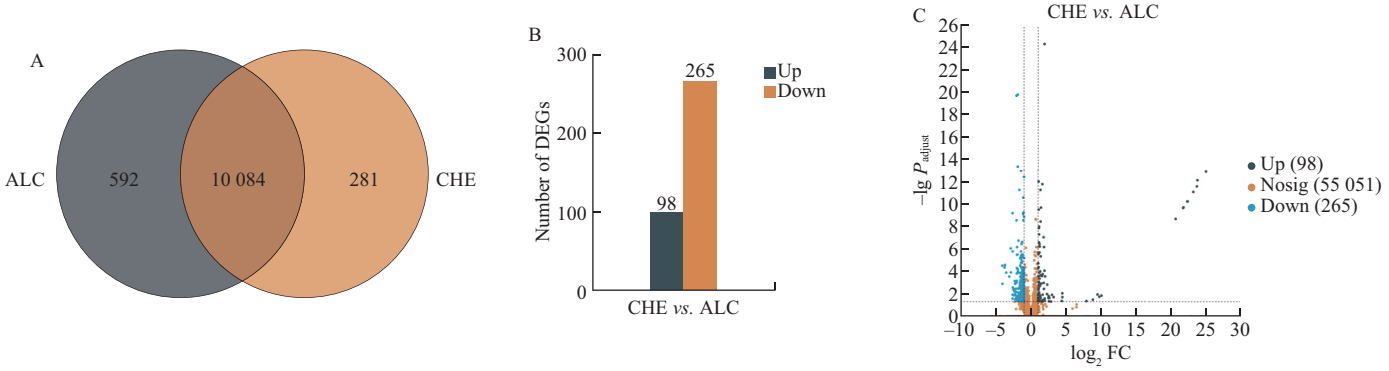

Fig. 5 Gut microbiota analysis. (A) Overlapping analysis. (B) PCoA on OTU level. (C) Community composition of gut microbiota at phylum level. (D) Community composition of gut microbiota at genus level. (E) Bar plots display the phylum-level distribution of gut microbiota in CHE and ALC groups. (F) Bar plots display the genus-level distribution of gut microbiota in CHE and ALC groups (95% CI). (G) Kruskal-Wallis H test was used to compare the relative abundance of some bacteria between CON, ALC and CHE groups.

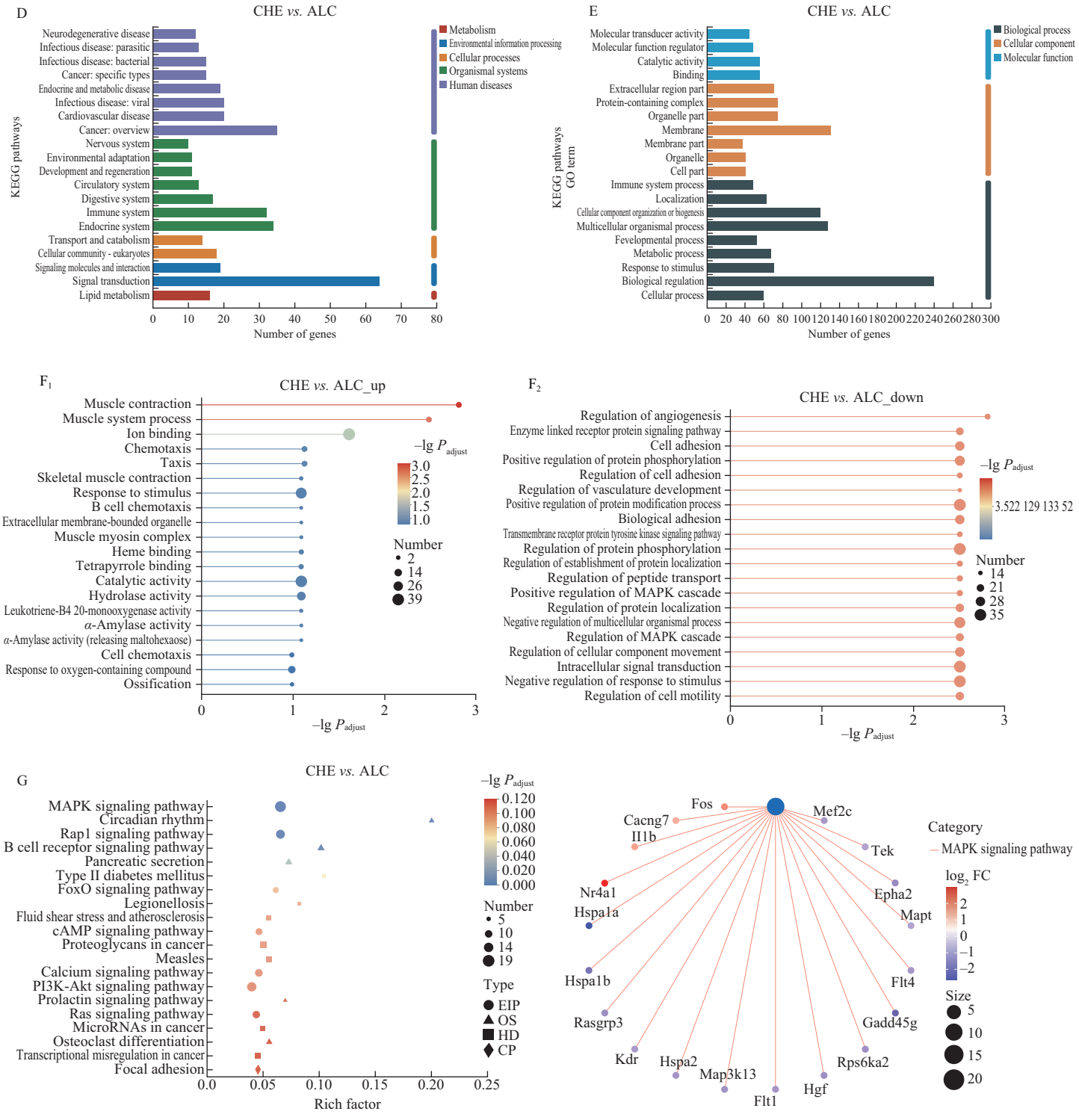

Fig. 5 (*Continued*)

Il1b. *Muribaculum* was negatively correlated with *Mef2c*, *Hspa1b*, *Hspa1a*, *Gadd45g*, *Tek*, *Flt4*, *Rps6ka2*, *Flt1*, *Kdr*. *Ruminococcus* was significantly positively correlated with *Mef2c*, *Hspa1b*, *Hspa1a*, *Epha2*, *Gadd45g*, *Hspa2*, *Flt4*, *Rps6ka2*, *Flt1*, and *Kdr* ($P < 0.05$). Additionally, *Eubacterium_xylanophilum*_group showed positive correlations with *Epha2* and *Gadd45g*. *Faecalibaculum* was negatively correlated with *Mapt*, *Epha2*, *Gadd45g*, *Rps6ka2*, and *Flt1*. *Helicobacter* was significantly positively correlated with *Flt4* ($P < 0.05$; Fig. 6B).

As shown in Fig. 6C, correlations of biochemical factors, microbiome and transcriptome were used to determine the association of biochemical factors, gut microbiota and genes. As shown in Fig. 6C, there are 13 bacteria commonly involved in BM and MT, namely *Allobaculum*, *Faecalibaculum*, *Helicobacter*, *Turicibacter,* norank_f_Oscillospiraceae, *Muribaculum*, *Clostridium_sensu_stricto*_1, *Candidatus_Saccharimonas*, unclassified_f_Oscillospiraceae, *Ruminococcus*, norank_f_norank_o_Clostridia_vadinBB60_group,

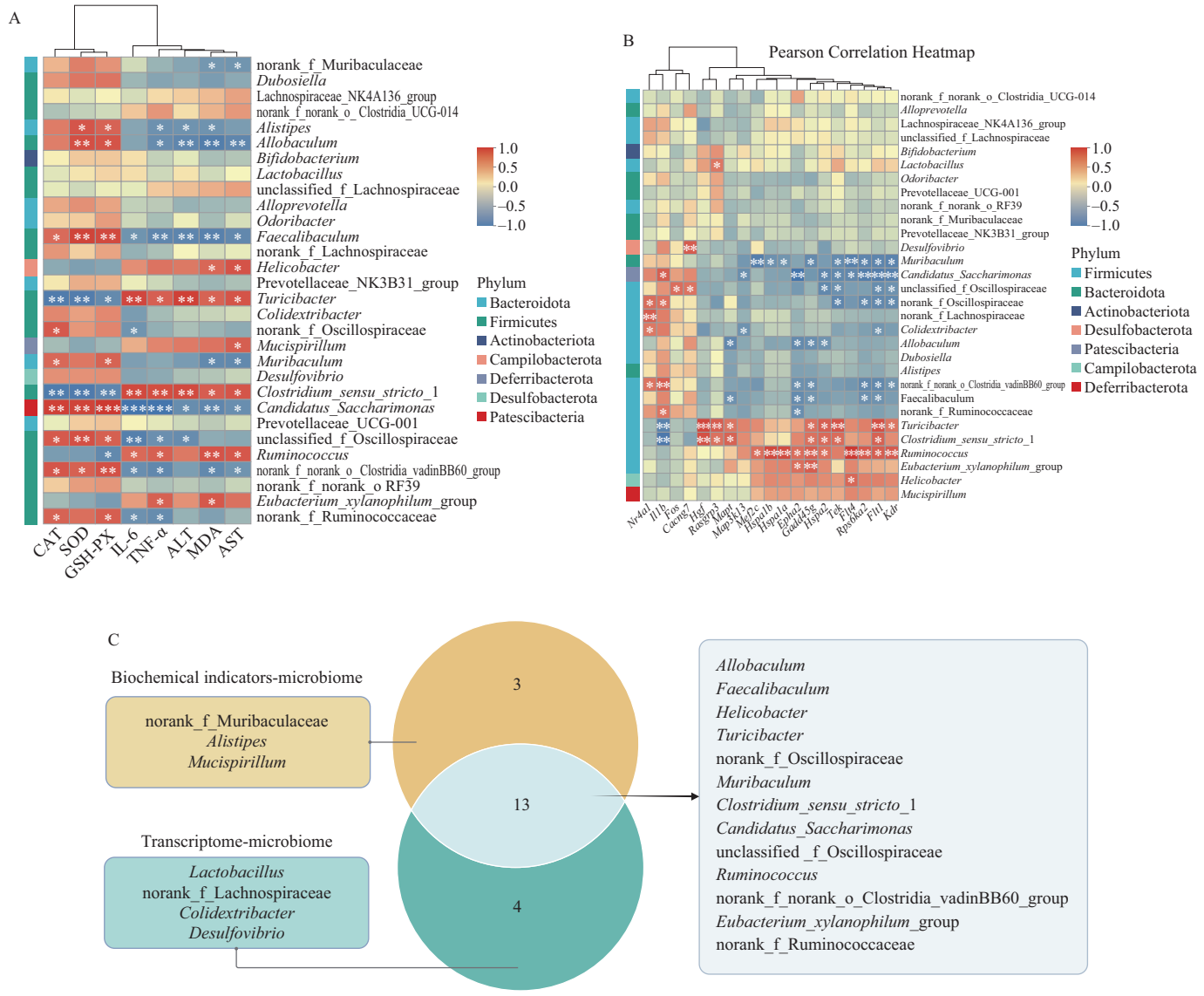

Fig. 6 Pearson correlation analysis. (A) Correlation analysis of biochemical markers-microbiome (BM). (B) Correlation analysis of microbiome-transcriptome (MT). (C) Venn diagram illustrating overlapping microbial taxa that exhibit significant associations in both BM and MT analyses.

*Eubacterium_xylanophilum*_group, and norank_f_Ruminococcaceae. The BM and MT correlation analysis revealed that the main bacteria they share are *Candidatus_Saccharimonas*, *Turicibacter* and *Clostridium_sensu_stricto*_1.

4. Discussion

Alcohol consumption represents a widespread component of contemporary lifestyle habits. However, excessive intake can exert detrimental effects on the body. Individuals with ALI exhibit distinct phenotypic alterations compared to healthy individuals, including changes in oxidative stress, inflammation, liver function, gut microbiota composition, and host gene expression. This study assessed the influence of CHE on mice with ALI and elucidated its potential hepatoprotective mechanisms.

SOD, GSH-PX, CAT, and MDA serve as key biomarkers of oxidative stress, reflecting the disruption of redox homeostasis between pro-oxidants and antioxidant defenses in biological systems. It has been reported that when excess ROS are released, the body's antioxidant system comes into play to scavenge ROS, resulting in lower levels of antioxidants in the body[14]. In this study, CHE upregulated key antioxidant enzymes (SOD, GSH-Px, and CAT) while suppressing MDA levels. IL-6 and TNF-α are well-recognized pro-inflammatory cytokines. Alcohol intake has been shown to disrupt intestinal barrier integrity, facilitating the translocation of LPS into the portal circulation, where it binds to carrier proteins and activates Kupffer cells, triggering pro-inflammatory cytokine release[15]. CHE suppressed alcohol-induced elevations of IL-6 and TNF-α, indicating its anti-inflammatory role in alleviating hepatic injury. Serum ALT and AST levels are established indicators of liver dysfunction severity. It has been shown that increased levels of ALT and AST are symptomatic of liver injury[16]. In this study, alcohol consumption led to increased ALT and AST levels, which were reversed by CHE, while liver tissue sections revealed that CHE reduced alcohol-induced inflammatory cell infiltration in the liver.

Additionally, drawing comparisons with previous report[9] and using the same control and experimental models, we evaluated the effects of CHE, *Puerariae Lobatae* Radix (PLR) alone versus

its combination with CHE in treating ALI. Interestingly, although the CHE-PLR combination remained effective in alleviating liver damage, its overall potency was lower than that of either individual treatment. This suggests a lack of synergistic effect and hints at a potential interference between the bioactive constituents of these 2 natural products (Fig. S2). This finding contrasts with the synergistic effects of the *Citri Reticulatae Pericarpium* and *Chaenomeles speciosa* (Sweet) *Nakai* (C + C) combination[12]. In that study, joint treatment significantly bolstered antioxidant defenses, yielding the lowest liver index and most pronounced reduction in serum TG. Conversely, our results suggest that the coexistence of CHE and PLR may lead to mutual interference rather than synergy. Notably, this discrepancy may stem not only from the inherent incompatibility between natural products but also from the variation in experimental durations across different batches. In this study, the 11-week intervention for the CHE + PLR group was substantially longer than the 8-week period in the C + C study. Such prolonged administration may have induced metabolic tolerance or cumulative physiological stress in the mice, leading to diminished long-term efficacy compared to individual natural products. This limitation underscores a crucial challenge: the unpredictable pharmacodynamic interactions and time-dependent adaptive responses of natural products. To explore strategies beyond simple blending, we previously developed a redox-responsive nanomicelle using HG-type pectin as a substrate to enhance the solubility and bioavailability of oleanolic acid (OA). Animal experiments demonstrated that this nanomicelle, PA-SS-OA, significantly mitigated ALI by activating the Nrf2 antioxidant pathway, exhibiting superior protection compared to OA[17]. These findings highlight that for natural products like CHE to achieve their maximum potential, future research could consider the advanced biopolymer-based delivery strategies over simple multi-component stacking, thereby ensuring consistent bioavailability and bypassing the unpredictable interactions often encountered in crude botanical combinations. It is worth noting that the intervention period for this nanomicelle study was only 6 weeks, which likely avoided the chronic adaptive responses associated with longer trials. These findings highlight that for natural products like CHE to achieve their maximum potential, future research should account for the critical impact of intervention duration on pharmacological outcomes. Furthermore, implementing advanced biopolymer-based delivery strategies over simple multi-component stacking could ensure consistent bioavailability within an optimal therapeutic window, thereby bypassing the unpredictable interactions and time-dependent metabolic interference often encountered in natural product combinations.

Alistipes have potential benefits for liver protection. One study reported that a reduction in *Alistipes* abundance occurs with the progression of decompensated cirrhosis[18], *Alistipes* abundance decreases in non-alcoholic steatohepatitis and cirrhosis patients[19-20]. Here, CHE tended to reverse the decrease of *Alistipes* abundance induced by ALC. In addition, Pearson analysis revealed *Alistipes* was positively associated with SOD but negatively linked to ALT and MDA. These data suggested that CHE may protect the liver by regulating the abundance of *Alistipes* to promote antioxidation and reduce the level of ALT. *Candidatus_Saccharimonas* is a beneficial bacterium that can differentiate between diabetic conditions and promote short-chain fatty acid production[21]. In the present study, CHE administration led to an increased abundance of *Candidatus_Saccharimonas*. Moreover, Pearson correlation analysis revealed significant negative associations between this genus and pro-inflammatory or oxidative stress markers (IL-6, TNF-α, MDA, ALT, and AST), while showing positive correlations with antioxidant enzymes (SOD, GSH-PX, and CAT). These data suggested that CHE protection of mice from alcohol-induced liver damage may be due to the interaction of *Candidatus_Ssacharmonas* with inflammatory factors and oxidative stress factors. One study reported that citrus peel powder has the function of increasing the abundance of *Faecalibaculum*[22], which is similar to our study. Therefore, multiple functional components in CHE may contribute to the increased relative abundance of *Faecalibaculum*. *Helicobacter* is a pathogenic Gram-negative bacteria. It has been reported that *Helicobacter* is considered to be the number one carcinogen of gastric cancer and can secrete many harmful substances such as urease, which can cause damage to the gastric mucosal barrier[23]. We observed a marked decrease in *Helicobacter* abundance in the ALC group relative to the CON group, aligning with prior studies reporting decreased *Helicobacter* prevalence in individuals with chronic alcohol intake[24]. A similar declining trend in *Helicobacter* abundance was also observed following CHE treatment. Although both CHE and ALC groups exhibited a tendency to reduce its abundance, alcohol consumption is associated with the onset of various diseases, whereas CHE supplementation may offer a safer intervention strategy. *Clostridium_sensu_stricto*_1 is a pathogenic bacterium whose abundance is associated with steatosis as well as inflammation[25]. Notably, *Clostridium_sensu_stricto*_1 exhibited significant positive correlations with pro-inflammatory cytokines IL-6 and TNF-α in the Pearson correlation analysis, corroborating findings from earlier research. *Turicibacter* is recognized as a pro-inflammatory bacterium, and previous studies have indicated that its increased abundance may be associated with oxidative stress, showing a positive correlation with MDA levels[26-27]. Here, we found that alcohol exposure significantly elevated the abundance of *Turicibacter*, whereas CHE treatment effectively restored it to near-normal levels. These findings suggest that CHE may alleviate inflammation and oxidative stress by modulating *Turicibacter* abundance, consequently mitigating liver injury. This is further supported by Pearson correlation analysis showing that *Turicibacter* positively correlates with inflammatory cytokines (IL-6, TNF-α) and negatively with antioxidant markers (SOD, GSH-PX, CAT). Therefore, CHE may reduce ALI by modulating the gut microbiota and mediating responses such as oxidative stress and inflammatory responses.

Network pharmacological analysis suggested a potential association between CHE-mediated amelioration of ALI and the MAPK signaling pathway, which was further corroborated by transcriptomic data. In this study, DEGs in the MAPK signaling pathway included *Mef2c*, *Tek*, *Epha2*, *Mapt*, *Flt4*, *Gadd45g*, *Rps6ka2*, *Hgf*, *Flt1*, *Map3k13*, *Hspa2*, *Kdr*, *Rasgrp3*, *Hspa1b*, *Hspa1a*, *Fos*, *Nr4a1*, *Il1b*, and *Cacng7*. Amelioration of ALI has been linked to suppression of oxidative stress and apoptosis *via* modulation of the MAPK signaling pathway[28-29]. Additionally, *Mef2c* overexpression has been shown to promote hepatocellular carcinoma cell proliferation, whereas its knockdown can counteract this effect[30]. *EphA2*, a member of the Eph receptor tyrosine kinase family, is considered a potential therapeutic target in cancer. Its involvement in modulating Wnt/*β*-catenin signaling plays a role in gastric cancer treatment[31]. *Hspa2* has been identified as a potential biomarker, showing

elevated expression in hepatocellular carcinoma and several other types of cancer[32]. CHE is rich in flavonoids such as quercetin, which has been shown to interact with HSPA2—a recognized molecular target—through binding mechanisms that contribute to its therapeutic potential in osteoarthritis[33]. *FLT-1*, *KDR* and *FLT-4* are members of the *VEGF* receptor family. Hepatic angiogenesis is associated with cirrhosis and *VEGF*, as a vascular endothelial growth factor, is usually present during the induction of hepatic angiogenesis[34]. Interestingly, beyond the receptors mentioned earlier, *Tie2* (also known as *Tek*) and *Tie1* have been highlighted as members of the receptor tyrosine kinase family specifically expressed in vascular endothelial cells[35]. *Gadd45g* upregulation correlates with non-alcoholic fatty liver disease (NAFLD) pathogenesis[36]. In addition, *Gadd45g* is thought to function as a promoter of cytokine secretion[37]. Decreased levels of *Mapt* are associated with attenuated neurotoxicity in Alzheimer's disease[38]. *RPS6KA2* downregulation has been shown to mitigate colitis, likely *via* MAPK pathway modulation[39]. *MAP3K13* is associated with the NF-κB signaling pathway that mediates inflammation[40]. *Hgf* has been shown to inhibit tumor progression by reducing angiogenesis[41]. *Rasgrp3* serves as a hepatocellular carcinoma proliferation marker, with its downregulation suppressing RAS activation and consequently inhibiting OKER cell proliferation[42]. *HSP70* is considered to be an inducer of pro-inflammatory factors due to its function in stimulating innate immune cells[43]. *Fos* deficiency has been shown to increase pro-inflammatory cytokines (TNF-α, IL-6, IL-12 p40) and reduce the anti-inflammatory cytokine IL-10 *in vivo* and *in vitro*[44]. *Nr4a1* is involved in maintaining hepatic lipid balance and possesses anti-inflammatory properties, contributing to the attenuation of hepatic steatosis[45].

Interestingly, GO enrichment analysis showed that regulation of angiogenesis and regulation of vasculature development were significantly enriched pathways for DEGs, which is consistent with KEGG enrichment analysis. This also reaffirmed that CHE attenuated ALI by inhibiting angiogenesis. Microbiome-transcriptome correlation analysis revealed strong associations between *Turicibacter*, *Clostridium_sensu_stricto_1*, and *Candidatus_Saccharimonas* and the MAPK signaling pathway. *Turicibacter* is a harmful bacterium that is often enriched in obese hosts[26,46], and can be detrimental to host health by increasing the promotion of inflammatory responses[27]. Alcohol intake markedly increases the abundance of *Clostridium_sensu_stricto_1* in the gut microbiota, which has been positively linked to IL-10[25]. Furthermore, the low abundance of *Clostridium_sensu_stricto_1* ameliorates colitis by downregulating the expression of inflammation-related genes[47]. *Candidatus_Saccharimonas* exhibits immunomodulatory properties, demonstrating a significant negative correlation with pro-inflammatory cytokines[48-49]. Transcriptomics implicated MAPK signaling genes primarily in angiogenic and inflammatory regulation. Notably, alcohol consumption has been found to stimulate angiogenesis, and angiogenesis is seen in liver diseases characterized by the phenotype of inflammation[50]. This may also explain why *Turicibacter*, *Clostridium_sensu_stricto_1* and *Candidatus_Saccharimonas* are associated with the MAPK signaling pathway. Therefore, it is reasonable that CHE can mediate the MAPK signaling pathway to reduce alcohol-induced liver inflammation and improve angiogenesis by modulating gut microbiota (Fig. 7). While this gut-liver axis mechanism is strongly supported by our integrated analyses, direct causal evidence at both the functional and protein levels is required for validation. Future validation should employ fecal microbiota transplantation (FMT) from CHE-treated mice, along with assessment of serum LPS and intestinal barrier markers, to cement the causal link from microbial remodeling to reduced endotoxin translocation. The role of the MAPK signaling pathway must be definitively confirmed through *in vivo* inhibition studies complemented by direct protein analysis, in order to fully delineate this protective cascade.

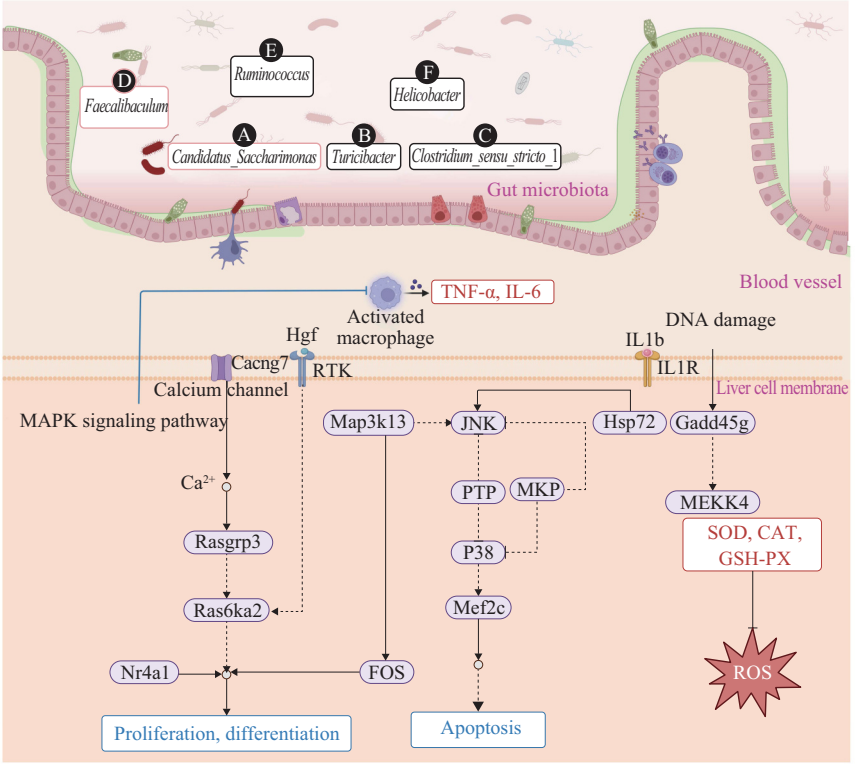

Fig. 7 Mechanism of CHE against ALI.

5. Conclusion

In summary, CHE demonstrates efficacy against ALI by not only restoring gut microbiota dysbiosis but also modulating the host MAPK signaling pathway, thereby ameliorating inflammation, oxidative stress, and liver tissue damage. It should be noted that the aforementioned mechanism is proposed based on multi-omics correlations, and its causal relationship requires further validation through gut microbiota transplantation and MAPK pathway inhibition experiments.

Conflict of interests

The authors declare no competing financial interests.

Acknowledgments

This work was financially supported by the National Natural Science Foundation of China (32201960, 32572622, 32330084), Yuelushan Laboratory Breeding Program (YLS-2025-ZY04029), Dongting Laboratory Special Funding Project (2025-DTYB-004), National Key Research and Development Program of China (2022YFD2100804).

Data availability statement

The raw data supporting the control and model groups in this study were derived from our previous report[9]. The 16S rRNA and transcriptome data are available from https://dataview.ncbi.nlm.nih.gov/object/PRJNA1010476?reviewer=nfvvnd7mn3nf54ssc9qgm0573o;https://dataview.ncbi.nlm.nih.gov/object/PRJNA1011968?reviewer=3chl9t8j4ae6nih4fqjglvh7j9;https://www.ncbi.nlm.nih.gov/bioproject/PRJNA1420460;https://www.ncbi.nlm.nih.gov/bioproject/PRJNA1420522.

Appendix A. Supplementary data

Supplementary data associated with this article can be found, in the online version, at http://doi.org/10.26599/FSHW.2026.9250939.

References

[1] M.F. Peng, Z.P. Gao, Y.F. Liao, et al., Development of citrus-based functional jelly and an investigation of its anti-obesity and antioxidant properties, Antioxidants 11 (2022) 2418. https://doi.org/10.3390/antiox11122418.

[2] M. Zhang, J.Y. Zhu, X. Zhang, et al., Aged citrus peel (*Chenpi*) extract causes dynamic alteration of colonic microbiota in high-fat diet induced obese mice, Food Funct. 11 (2020) 2667-2678. https://doi.org/10.1039/c9fo02907a.

[3] J.J. Guo, H.L. Tao, Y. Cao, et al., Prevention of obesity and type 2 diabetes with aged citrus peel (*Chenpi*) extract, J. Agric. Food Chem. 64 (2016) 2053-2061. https://doi.org/10.1021/acs.jafc.5b06157.

[4] F. Zhou, Y.-L. Li, X. Zhang, et al., Polyphenols from Fu brick tea reduce obesity *via* modulation of gut microbiota and gut microbiota-related intestinal oxidative stress and barrier function, J. Agric. Food Chem. 69 (2021) 14530-14543. https://doi.org/10.1021/acs.jafc.1c04553.

[5] W.H. Organization. Global status report on alcohol and health and treatment of substance use disorders. Geneva: World Health Organization; 2024.

[6] J. Hyun, J. Han, C. Lee, et al., Pathophysiological aspects of alcohol metabolism in the liver, Int. J. Mol. Sci. 22 (2021) 5717. https://doi.org/10.3390/ijms22115717.

[7] P. Zhang, K. Watari, M. Karin, Innate immune cells link dietary cues to normal and abnormal metabolic regulation, Nat. Immunol. 26 (2025) 29-41. https://doi.org/10.1038/s41590-024-02037-y.

[8] Y.P. Ru, J. Jia, X.Y. Yang, et al., From bugs to behavior: targeting the gut-brain interface for addiction therapeutics, Gut Microbes 17 (2025) 2569740. https://doi.org/10.1080/19490976.2025.2569740.

[9] Y.F. Liao, J.J. Guo, Z.P. Gao, et al., *Puerariae lobatae* radix alleviates alcoholic liver injury by regulating circadian rhythm and intestinal flora, Food Front. 6(5)(2025) 2281-2294. https://doi.org/10.1002/fft2.70021.

[10] C. Wang, Z.P. Gao, Y.J. Qian, et al., Effects of different concentrations of ganpu tea on fecal microbiota and short chain fatty acids in mice, Nutrients 13 (2021) 3715. https://doi.org/10.3390/nu13113715.

[11] X. Wang, Z.P. Su, X. Li, et al., Targeted/untargeted metabolomics and antioxidant properties distinguish *Citrus reticulata* 'Chachi' from *Citrus reticulata* Blanco, Food Chem. 462 (2025) 140806. https://doi.org/10.1016/j.foodchem.2024.140806.

[12] S.S. Ma, L.T. Kang, Z.P. Gao, et al., Hepatoprotective effects of *Citri reticulatae* Pericarpium and *Chaenomelese speciosa* (Sweet) Nakai extracts in alcohol-related liver injury: modulation of oxidative stress, lipid metabolism, and gut microbiota, Antioxidants 14 (2025) 343. https://doi.org/10.3390/antiox14030343.

[13] Y.F. Liao, C. Wang, Z.P. Gao, et al., The anti-obesity mechanism of Ganpu tea revealed by microbiome, metabolome, and transcriptome analysis, Food Chem. 412 (2022) 135048. https://doi.org/10.1016/j.foodchem.2022.135048.

[14] L.Y. Wang, L. Ding, Z.P. Yu, et al., Intracellular ROS scavenging and antioxidant enzyme regulating capacities of corn gluten meal-derived antioxidant peptides in HepG2 cells, Food Res. Int. 90 (2016) 33-41. https://doi.org/10.1016/j.foodres.2016.10.023.

[15] T. Uesugi, M. Froh, G.E. Arteel, et al., Role of lipopolysaccharide-binding protein in early alcohol-induced liver injury in mice, J. Immunol. 168 (2002) 2963-2969. https://doi.org/10.4049/jimmunol.166.7.4737.

[16] L. Zhao, Y. Wang, J. Liu, et al., Protective effects of genistein and puerarin against chronic alcohol-induced liver injury in mice *via* antioxidant, anti-inflammatory, and anti-apoptotic mechanisms, J. Agric. Food Chem. 64 (2016) 7291-7297. https://doi.org/10.1021/acs.jafc.6b02907.

[17] L. Kang, X. Chang, S. Ma, et al., Redox-responsive self-assembled HG-type pectin nanomicelles for alleviating chronic alcoholic liver injury in mice, Carbohydr. Polym. 361 (2025) 123619. https://doi.org/10.1016/j.carbpol.2025.123619.

[18] B.J. Parker, P.A. Wearsch, A.C. Veloo, et al., The genus *Alistipes*: gut bacteria with emerging implications to inflammation, cancer, and mental health, Front. Immunol. 11 (2020) 906. https://doi.org/10.3389/fimmu.2020.00906.

[19] N. Qin, F.L. Yang, A. Li, et al., Alterations of the human gut microbiome in liver cirrhosis, Nature 513 (2014) 59-64. https://doi.org/10.1038/nature13568.

[20] M. Rau, A. Rehman, M. Dittrich, et al., Fecal SCFAs and SCFA-producing bacteria in gut microbiome of human NAFLD as a putative link to systemic T-cell activation and advanced disease, United Eur. Gastroenterol. J. 6 (2018) 1496-1507. https://doi.org/10.1177/2050640618804444.

[21] L.M. Luo, J.L. Luo, Y.T. Cai, et al., Inulin-type fructans change the gut microbiota and prevent the development of diabetic nephropathy, Pharmacol. Res. 183 (2022) 106367. https://doi.org/10.1016/j.phrs.2022.106367.

[22] M.Y. Hu, L. Zhang, Z. Ruan, et al., The regulatory effects of citrus peel powder on liver metabolites and gut flora in mice with non-alcoholic fatty liver disease (NAFLD), Foods 10 (2021) 3022. https://doi.org/10.3390/foods10123022.

[23] J.D. Zeng, C. Xie, L. Zhang, et al., Host cell antimicrobial responses against *Helicobacter pylori* infection: from biological aspects to therapeutic strategies, Int. J. Mol. Sci. 23 (2022) 10941. https://doi.org/10.3390/ijms231810941.

[24] P.Q. Du, C. Zhang, A.F. Wang, et al., Association of alcohol drinking and *Helicobacter pylori* infection: a meta-analysis, J. Clin. Gastroenterol. 57 (2023) 269-277. https://doi.org/10.1097/MCG.0000000000001638.

[25] Z.W. Yi, X.F. Liu, L.H. Liang, et al., Antrodin A from *Antrodia camphorata* modulates the gut microbiome and liver metabolome in mice exposed to acute alcohol intake, Food Funct. 12 (2021) 2925-2937. https://doi.org/10.1039/d0fo03345f

[26] T.T. Li, Z.R. Huang, R.B. Jia, et al., *Spirulina platensis* polysaccharides attenuate lipid and carbohydrate metabolism disorder in high-sucrose and high-fat diet-fed rats in association with intestinal microbiota, Food Res. Int. 147 (2021) 110530. https://doi.org/10.1016/j.foodres.2021.110530.

[27] L.L. Yu, L.Y. Zhang, H. Duan, et al., The protection of *Lactiplantibacillus plantarum* CCFM8661 against benzopyrene-induced toxicity *via* regulation of the gut microbiota, Front. Immunol. 12 (2021) 736129. https://doi.org/10.3389/fimmu.2021.736129.

[28] D.D. Ma, Z.Y. Wang, Z.Y. He, et al., Pine pollen extract alleviates ethanol-induced oxidative stress and apoptosis in HepG2 cells *via* MAPK signaling, Food Chem. Toxicol. 171 (2023) 113550. https://doi.org/10.1016/j.fct.2022.113550.

[29] S. Rezatabar, A. Karimian, V. Rameshknia, et al., RAS/MAPK signaling functions in oxidative stress, DNA damage response and cancer progression, J. Cell. Physiol. 234 (2019) 14951-14965. https://doi.org/10.1002/jcp.28334.

[30] H. Zhang, W. Liu, Z. Wang, et al., MEF2C promotes gefitinib resistance in hepatic cancer cells through regulating MIG6 transcription, Tumori J. 104 (2018) 221-231. https://doi.org/10.1177/0300891618765555.

[31] Q. Peng, L. Chen, W. Wu, et al., EPH receptor A2 governs a feedback loop that activates Wnt/β-catenin signaling in gastric cancer, Cell Death Dis. 9 (2018) 1-16. https://doi.org/10.1038/s41419-018-1164-y.

[32] Y. Fu, H. Zhao, X.S. Li, et al., Expression of HSPA2 in human hepatocellular carcinoma and its clinical significance, Tumor Biol. 35 (2014) 11283-11287. https://doi.org/10.1007/s13277-014-2430-y.

[33] D.J. Ma, T. Yu, L.P. Peng, et al., PIM1, CYP1B1, and HSPA2 targeted by quercetin play important roles in osteoarthritis treatment by *Achyranthes bidentata*, EVID-BASED COMPLALT. 2019 (2019) 1-10. https://doi.org/10.1155/2019/1205942.

[34] J. Medina, A.G. Arroyo, F. Sánchez-Madrid, et al., Angiogenesis in chronic inflammatory liver disease, Hepatology 39 (2004) 1185-1195. https://doi.org/10.1002/hep.20193.

[35] C. Suri, P.F. Jones, S. Patan, et al., Requisite role of angiopoietin-1, a ligand for the TIE2 receptor, during embryonic angiogenesis, Cell 87 (1996) 1171-1180. https://doi.org/10.1016/s0092-8674(00)81813-9.

[36] R.M. Wang, L.L. Yao, X. Lin, et al., Exploring the potential mechanism of *Rhodomyrtus tomentosa* (Ait.) Hassk fruit phenolic rich extract on ameliorating nonalcoholic fatty liver disease by integration of transcriptomics and metabolomics profiling, Food Res. Int. 151 (2022) 110824. https://doi.org/10.1016/j.foodres.2021.110824.

[37] Y.H. Nam, I. Rodriguez, S.Y. Jeong, et al., Avocado oil extract modulates auditory hair cell function through the regulation of amino acid biosynthesis genes, Nutrients 11 (2019) 113. https://doi.org/10.3390/nu11010113.

[38] U.C. Dash, S.K. Swain, S. Kanhar, et al., The modulatory role of prime identified compounds in *Geophila repens* in mitigating scopolamine-induced neurotoxicity in experimental rats of Alzheimer's disease *via* attenuation of cholinesterase, β-secretase, MAPt levels and inhibition of oxidative stress imparts inflammation, J. Ethnopharmacol. 282 (2022) 114637. https://doi.org/10.1016/j.jep.2021.114637.

[39] H. Kim, N. Banerjee, I. Ivanov, et al., Comparison of anti-inflammatory mechanisms of mango (*Mangifera indica* L.) and pomegranate (*Punica Granatum* L.) in a preclinical model of colitis, Mol. Nutr. Food Res. 60 (2016) 1912-1923. https://doi.org/10.1002/mnfr.201501008.

[40] R. Kawata, S. Oda, Y. Koya, et al., Macrophage-derived extracellular vesicles regulate concanavalin A-induced hepatitis by suppressing macrophage cytokine production, Toxicology. 443 (2020) 152544. https://doi.org/10.1016/j.tox.2020.152544

[41] H. Koizumi, T. Yamada, S. Takeuchi, et al., Hsp90 inhibition overcomes HGF-triggering resistance to EGFR-TKIs in EGFR-mutant lung cancer by decreasing client protein expression and angiogenesis, J. Thorac. Oncol. 7 (2012) 1078-1085. https://doi.org/10.1097/JTO.0b013e3182519a2c

[42] T.C. Delgado, F. Lopitz-Otsoa, M.L. Martínez-Chantar, Post-translational modifiers of liver kinase B1/serine/threonine kinase 11 in hepatocellular carcinoma, J. Hepatocell. Carcinoma 6 (2019) 85. https://doi.org/10.2147/JHC.S169585.

[43] H.Y. Liu, X.L. Pei, J. Wang, et al., Effect of loach paste on the liver and immune organs of *D*-galactose-induced ageing mice, Food Agric. Immunol. 29 (2018) 316-331. https://doi.org/10.1080/09540105.2017.1376037.

[44] N. Ray, M. Kuwahara, Y. Takada, et al., c-Fos suppresses systemic inflammatory response to endotoxin, Int. Immunol. 18 (2006) 671-677. https://doi.org/10.1093/intimm/dxl004.

[45] H.J. Liang, X.N. Xie, X.H. Song, et al., Orphan nuclear receptor NR4A1 suppresses hyperhomocysteinemia-induced hepatic steatosis *in vitro* and *in vivo*, FEBS Lett. 593 (2019) 1061-1071. https://doi.org/10.1002/1873-3468.13384.

[46] X.B. Yang, W.J. Mo, C.J. Zheng, et al., Alleviating effects of noni fruit polysaccharide on hepatic oxidative stress and inflammation in rats under a high-fat diet and its possible mechanisms, Food Funct. 11 (2020) 2953-2968. https://doi.org/10.1039/d0fo00178c.

[47] X. Wen, H.G. Wang, M.N. Zhang, et al., Fecal microbiota transplantation ameliorates experimental colitis *via* gut microbiota and T-cell modulation, World J. Gastroenterol. 27 (2021) 2834. https://doi.org/10.3748/wjg.v27.i21.2834.

[48] H.F. Ge, Z.Z. Cai, J.L. Chai, et al., Egg white peptides ameliorate dextran sulfate sodium-induced acute colitis symptoms by inhibiting the production of pro-inflammatory cytokines and modulation of gut microbiota composition, Food Chem. 360 (2021) 129981. https://doi.org/10.1016/j.foodchem.2021.129981.

[49] Q.W. Lin, M.Y. Liu, G.G.L. Yue, et al., Anti-inflammatory activities of natural cyclopeptide RA-XII in colitis-associated colon cancer mouse model and its effect on gut microbiome, Phytother. Res. 36 (2022) 2641-2659. https://doi.org/10.1002/ptr.7482.

[50] H. Kawaratani, K. Moriya, T. Namisaki, et al., Therapeutic strategies for alcoholic liver disease: focusing on inflammation and fibrosis, Int. J. Mol. Med. 40 (2017) 263-270. https://doi.org/10.3892/ijmm.2017.3015.